ISSN 2229-5518

Behavior of Integral Abutment Bridge with and without Soil Interaction

R.Shreedhar, Vinod Hosur, Iftikar Chappu

Abstract— Integral Abutment bridges (IAB's) can be defined as bridges without joints. The main purpose of constructing IAB's is to prevent the corrosion of the structure due to water seepage through joints. The biggest uncertainty in the design of these bridges is the reaction of the soil behind the abutments and next to the foundation piles, especially during thermal expansion. This lateral soil reaction is nonlinear and is a function of the magnitude and nature of the wall displacement.To gain a better understanding of the mechanism of load transfer due to thermal expansion, which is also dependent on the type of the soil adjacent to the abutment walls and piles, a 3D finite element analysis is carried out on representative IAB. In this paper two models are compared one with considering soil interaction and other without soil interaction and live load is applied using STAAD-Beava. The main objective is to study the trends in bending moment, shear force and deflection in central and end longitudinal girders and deck slab due to dead load, live load in combination of thermal loads. This paper emphysis that the temperature effects are more significant in case of integral abutment bridges, however the changes in soil properties behind the abutment and around the piles do not affect significantly the performance of super structure.

Index Terms— Abutment, Deck, Integral Bridge, Piles, Soil interaction, Springs, Thermal stresses.

1 Introduction

INTEGRAL Abutment bridges (IAB's) are the bridges without joints. Bearings and expansion joints are the weak links in a bridge. Hence, interest in integral bridges or joint less bridge is increasing and their performance has gained international attention. The main purpose of constructing IAB's is to prevent the corrosion of the structure due to water seepage through joints. The simple and rapid construction provides smooth, uninterrupted deck that is aesthetically pleasing and safer for riding.

The continuity achieved by this construction results in thermally induced deformations. These in turn introduce a significantly complex and non-linear soil structure interaction into the response of abutment walls and piles of the IAB. The unknown soil response and its effect on the stresses in the bridge, creates uncertainties in the design.

To gain a better understanding of the mechanism of load transfer due to thermal expansion, which is also dependent on the type of the soil adjacent to the abutment walls and piles, a 3D finite element analysis is carried out on representative IAB using software STAAD ProV8i and live load was introduced as per IRC-6(2000) using STAAD-Beava (Bridge Engineering Automated Vehicle Application). The nonlinear soil behaviour is handled using multilinear springs at the abutment wall and pile nodes. The nonlinear soil springs behind the walls are the force-deflection design curves recommended in the National Cooperative Highways Research Program (NCHRP 1991) design manual. The nonlinear p-y design curves recommended by the American Petroleum Institute (API 1993) are used adjacent to the piles.

- Prof. R. Shreedhar is associate professor in the Department of Civil engineering in Gogte Institute of Technology Belgaum (Karnataka), INDIA, PH:+919845005722. E-mail: rshree2006@gmail.com
- Dr.Vinod Hosur Professor in the Department of Civil Engineering at Gogte Institute of Technology Belgaum (Karnataka), INDIA, Ph:+919448193110. E-mail: vinod.hosur@gmail.com
- Iftikar S Chappu is currently pursuing master degree in Structural engineering at Gogte Institute of Technology Belgaum (Karnataka), INDIA, PH:+919742084390. E-mail: iftikar.sc@gmail.com

2 Numerical Example:

The objective of the present work is to study the behaviour of the integral bridge under various load combinations of dead load, live load and thermal loads varying from 10^0C to 50^0C with 10°C rise with each load case applied throughout the bridge deck in the longitudinal direction. The live load is applied as per IRC 6- 2000 using STAAD-Beava (Bridge Engineering Automated Vehicle Application). Here the software automatically calculates the vehicle load and no of lanes depending upon the carriage way width as per the codal provision.

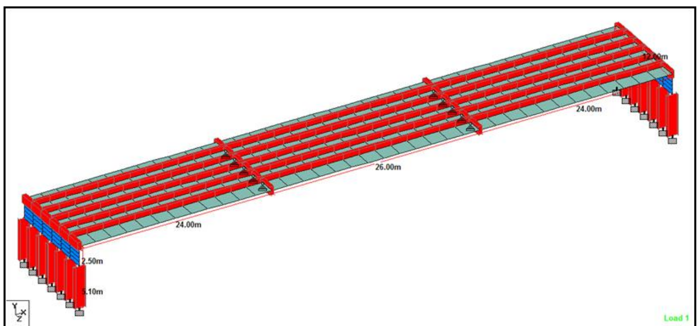

Fig. 1. Picture showing the model of IAB

Deck Slab:- *Length:74 mt; Width:12mt; Thickness:0.24mt*
Abutment:- *Height 2.5mt; Width:12mt; Thickness:1.25mt*
Girders:- *Longitudinal girder: 5 nos (0.35mt X 1.5mt)*
Cross girder: 4 nos (0.5mt X 1.0mt)
Piles:- *Nos 7; Height: 5.1mt*

3 Structural and Material Modelling of an Integral Bridge

The structural elements of the bridge are modeled as linear elements while the soil reaction adjacent to the piles and behind the abutment walls are modeled as nonlinear support springs. The 3D model of the structure comprises of:

i. The superstructure consisting of concrete slab acting in composition with five longitudinal girders and four cross beams, one at each end of span.
ii. The deck slab is modeled using plate elements and the girders as beam elements. The intermediate piers being treated as simple roller supports.
iii. The 2.5 m high abutment modeled as plate elements. The soil behind the abutment and around the piles modeled as multilinear springs.
iv. Seven steel piles with full fixity are connected to each abutment walls, allowing full moment transfer. Each pile is modeled as beam element with common node for pile and the abutment wall using structural analysis software, STAAD.Pro V8i.

4 Calculation of Spring Stiffness for Abutment and Piles

4.1 Spring Stiffness Calculations for Abutment

NCHRP curves relate the horizontal normal stress σ'_h to the vertical effective normal stress σ'_v according to $\sigma'_h = K\ \sigma'_v$ where for a uniform density dry soil $\sigma'_v = \gamma z$, where γ = dry density of soil.

To calculate the effective soil spring resistance for input into the bridge model, the effective panel size of each wall element is computed using dimension as used in the model. Typical interior panels are of width w =2m and height h= 0.5m. this area is multiplied by the effective vertical normal stress σ'_v for a given panel depth z and by the lateral earth pressure coefficient K for a given deflection to yield a lateral force – deflection curve for a given node $F = K\ \sigma'_v\ w\ h$ (6)

Where $\sigma'_v = \gamma z$
σ'_v = vertical normal stress
z = panel depth
w = width of plate as used in model
h= height of plate as used in model
K=Earth pressure coefficient versus relative wall displacement

4.2 Spring Stiffness Calculation for Piles

As earlier stated the soil resistance p is given by equation

$$p = tanh\left[\frac{k1z}{A\ pu}\ y\right] A\ pu$$

And the force-displacement relation is given by

$$F = A\ pu\ \tanh\left(\frac{k1zy}{Apu}\right) Lp \qquad (6)$$

Where,
A= 0.9 is introduced for cyclic loading (= 3.0 − 0.8 (z/D) ≥ 0.9)
F= force in spring
p_u = ultimate soil resistance (lower of p_{us} or p_{ud})
p_{us} = shallow ultimate resistance
p_{ud} = deep ultimate resistance
k_1 = initial soil stiffness chosen for a given of friction Φ
z = soil depth from the bottom of approach slab to the spring
y = horizontal displacement
L_p = length of beam element

The ultimate soil resistances are given as
$p_{us} = (c_1 z + c_2 D)\ \gamma' z$
$p_{ud} = c_3 \gamma' D z$
where,
γ' = dry density of soil adjacent to piles
Φ = angle of internal friction in sand
c_1, c_2, and c_3 are coefficients as functions of Φ, and
D = average pile diameter from surface to depth (length).
$c_1 = k_0 \tan(\phi) \sin\beta / \tan(\beta - \phi) \cos(\alpha) + \tan^2\beta \tan(\alpha) / \tan(\beta-\phi) + k_0 \tan\beta(\tan(\phi) \sin\beta - \tan(\alpha))$
$c_2 = \tan\beta / \tan(\beta-\phi) - \tan^2(45-\phi/2)$
$c_3 = k_0 \tan(\phi) \tan^4\beta + k_a (\tan^8\beta - 1)$
$\alpha = \Phi/2$
$\beta = 45 + \Phi/2$
k_o= at rest earth pressure coefficient = $(1-\sin\Phi)$
k_a= Rankine active earth pressure coefficient = $\tan^2(45-\Phi/2)$
Initial stiffness of soil= k_1
Dry density of soil adjacent to piles = γ'

5 Results and Discussion

The results are compared for the bending moments, deflection and shear force for the central and end longitudinal girder and deck slab and are presented in the form of graphs considering the effects of soil for IAB's.

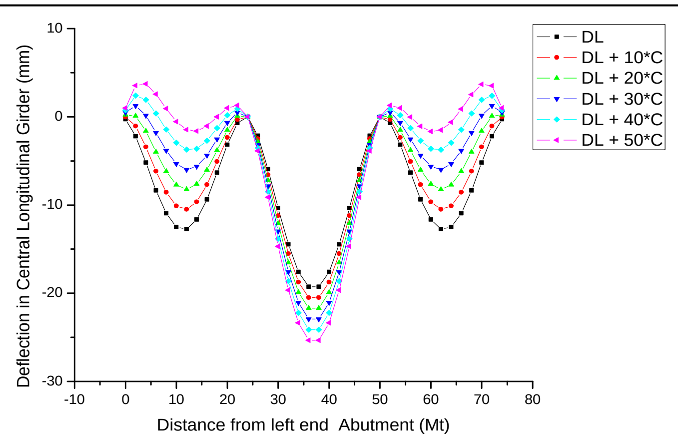

Fig. 1. Deflection in central longitudinal girder due to dead load + thermal load combination of IAB with soil interaction

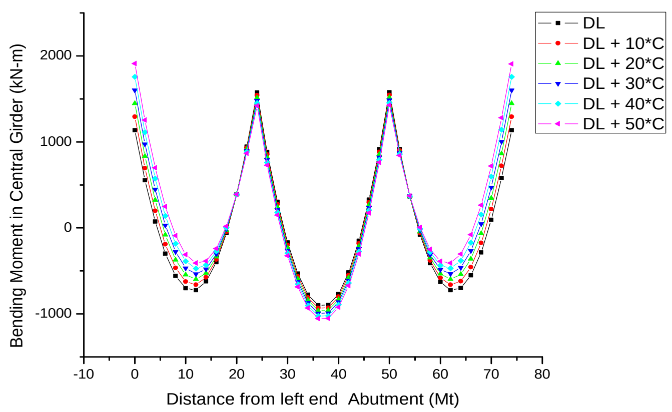

Fig. 2. Bending moment in central longitudinal girder due to dead load + thermal load combination of IAB with soil interaction.

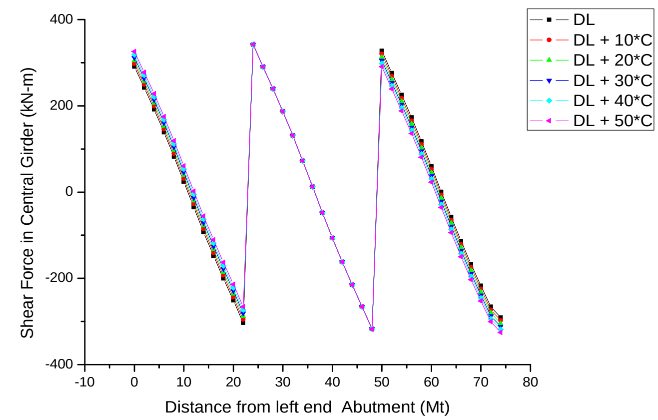

Fig. 3. Shear force in central longitudinal girder due to dead load + thermal load combination of IAB with soil interaction.

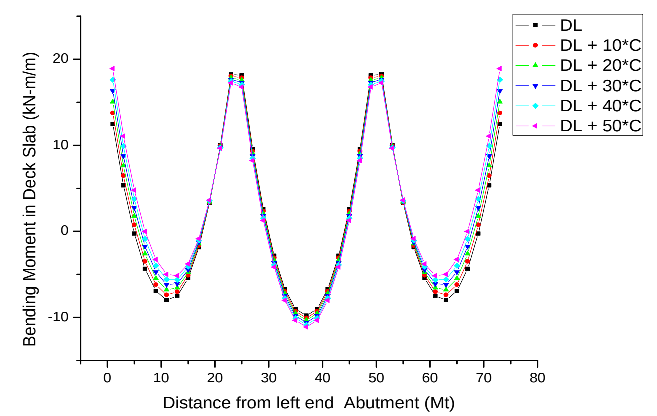

Fig. 4. Bending moment in deck slab due to dead load + thermal load combination of IAB with soil interaction.

The variation of bending moment, shear force and deflection in longitudinal girders is found to increases with increase in temperature.

The maximum percentage variation in Deflection in longitudinal girder due to Dead load + Thermal load for IAB with soil interaction for 10⁰C to 50⁰C is 6.3% to 31.5%. (Fig. 1)

There is significant variation in bending moment in the longitudinal girder due to increase in temperature. The maximum percentage variation in bending moment due to Dead load + Thermal load for IAB with soil interaction is obtained to be around 14% for 10⁰C and 68% for 50⁰C. (Fig 2)

The maximum percentage variation in shear force due to Dead load + Thermal load for IAB with soil interaction is obtained to be around 2.4% for 10⁰C and 12% for 50⁰C. (Fig 3)

The maximum percentage variation in bending moment in deck slab due to Dead load + Thermal load for IAB with soil interaction is obtained to be around 14% for 10⁰C and 71% for 50⁰C. (Fig 4)

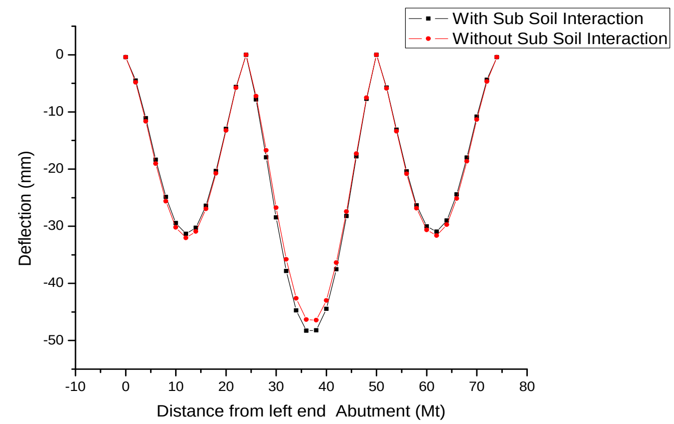

Fig. 5. Comparison of deflection in central longitudinal girder due to dead load + live load for IAB's with and without Soil Interaction

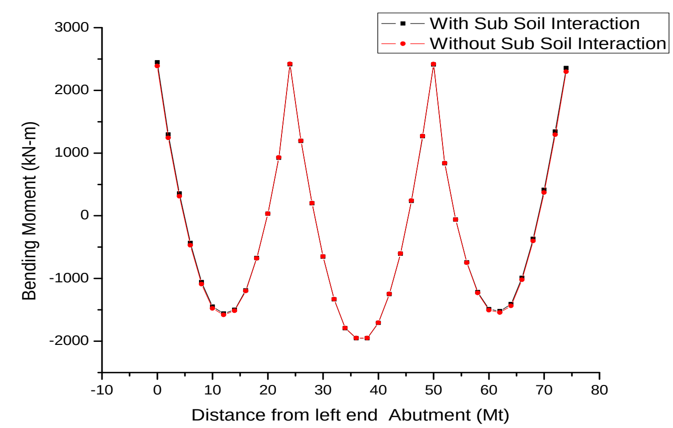

Fig. 6. Comparison of bending moment in central longitudinal girder due to dead load + live load for IAB's with and without Soil Interaction

The reduction in the maximum deflection due to Dead load + Live load in the girders for the IAB without soil interaction as compared to IAB with soil interaction are 2.54% & 4.02% for end & central longitudinal girder respectively. (Fig 5)

The maximum positive moments due to Dead load + Live load in the girders for the IAB without soil interaction are slightly lower than the IAB with soil interaction. For the two bridges considered in the study, the reduction in the maximum positive moment are 1.57% and 2.47% for end & central longitudinal girder respectively. (Fig 6)

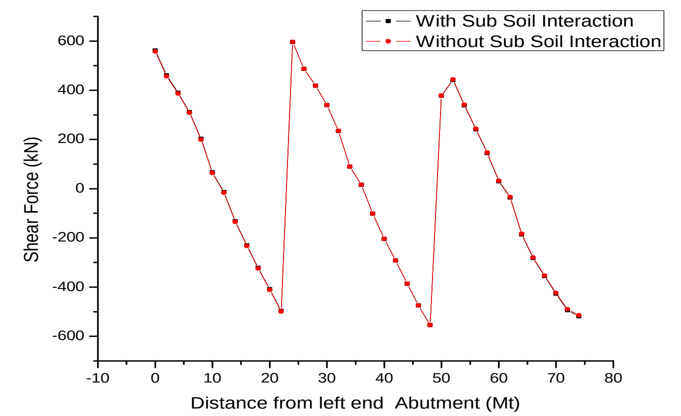

Fig. 7. Comparison of shear force in central longitudinal girder due to dead load + live load for IAB's with and without Soil Interaction

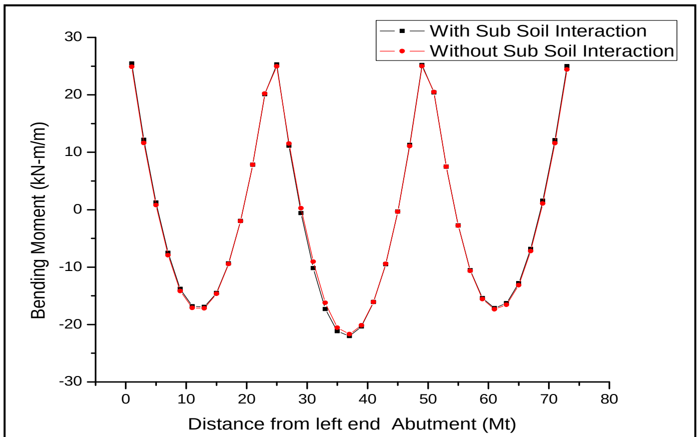

Fig. 8. Comparison of bending moment in deck slab due to dead load + live load for IAB's with and without Soil Interaction

The reduction in the maximum deflection due to Dead load + Live load in the girders for the IAB without soil interaction as compared to IAB with soil interaction are 2.54% & 4.02% for end & central longitudinal girder respectively. (Fig 5)

The maximum positive moments due to Dead load + Live load in the girders for the IAB without soil interaction are slightly lower than the IAB with soil interaction. For the two bridges considered in the study, the reduction in the maximum positive moment are 1.57% and 2.47% for end & central longitudinal girder respectively. (Fig 6)

There is negligible difference in the maximum Shear Force due to Dead load + Live load in the girders for the IAB without soil interaction as compared to IAB with soil interaction i.e. 0.14% & 0.72% for end & central longitudinal girder respectively. (Fig 7)

The maximum positive moments due to Dead load + Live load in the Deck Slab for the IAB without soil interaction are slightly lower than the IAB with soil interaction. For the two bridges considered in the study, the reduction in the maximum positive moment in the bridge deck is 2.27%. (Fig 8)

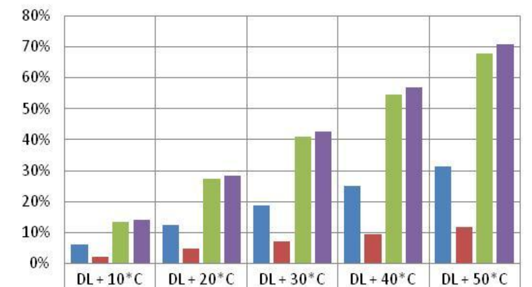

	DL + 10°C	DL + 20°C	DL + 30°C	DL + 40°C	DL + 50°C
Defln in Central Girder	6.31%	12.61%	18.92%	25.22%	31.47%
SF in Central Girder	2.41%	4.82%	7.23%	9.64%	12.05%
BM in Central Girder	13.64%	27.28%	40.93%	54.50%	67.73%
BM in Deck Slab	14.22%	28.43%	42.66%	56.84%	70.77%

Fig. 9. Percentage variation of Deflection, SF & BM of IAB with soil interaction for Dead Load and Combination of Thermal Load.

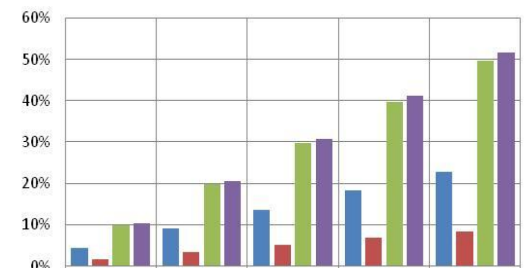

	DL + 10°C	DL + 20°C	DL + 30°C	DL + 40°C	DL + 50°C
Defln in Central Girder	4.60%	9.19%	13.79%	18.38%	22.97%
SF in Central Girder	1.72%	3.43%	5.15%	6.87%	8.58%
BM in Central Girder	9.97%	19.95%	29.92%	39.90%	49.87%
BM in Deck Slab	10.33%	20.67%	30.99%	41.33%	51.66%

Fig. 10. Percentage variation of Deflection, SF & BM of IAB without soil interaction for Dead Load and Combination of Thermal Load.

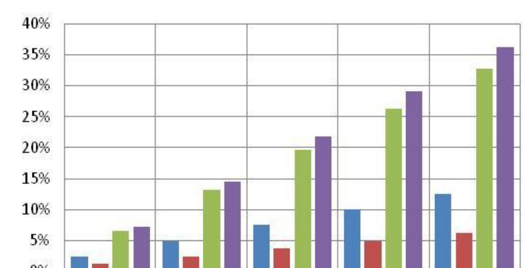

	DL+LL+10°C	DL+LL+20°C	DL+LL+30°C	DL+LL+40°C	DL+LL+50°C
Defln in Central Girder	2.52%	5.03%	7.55%	10.07%	12.56%
SF in Central Girder	1.25%	2.50%	3.75%	4.99%	6.25%
BM in Central Girder	6.58%	13.16%	19.74%	26.29%	32.67%
BM in Deck Slab	7.26%	14.52%	21.79%	29.03%	36.15%

Fig. 11. Percentage variation of deflection, SF & BM of IAB with soil interaction for dead load + live load and Combination of Thermal Load.

ISSN 2229-5518

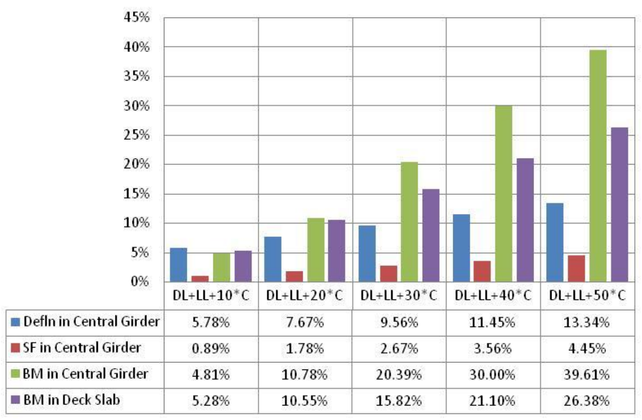

Fig. 12. Percentage variation of deflection, SF & BM of IAB without soil interaction for dead load + live load and Combination of Thermal

TABLE 1
PERCENTAGE CHANGE FOR IAB WITH SOIL INTERACTION WITH RESPECT TO IAB WITHOUT SOIL INTERACTION FOR DEAD LOAD CONDITION

		Difference		% Change
Deflection	End Girder	0.20	mm	0.83
	Central Girder	0.19	mm	1.00
Shear Force in Longitudinal Girders	End Girder	0.55	kN	0.15
	Central Girder	1.82	kN	0.63
Bending Moment in Longitudinal Girders	End Girder	-23.0	kN-m	1.52
	Central Girder	-29.4	kN-m	2.59
Bending Moment in Deck Slab	End Plate	-0.3	kN-m/m	2.29
	Centre Plate	0.1	kN-m/m	0.60

TABLE 2
PERCENTAGE CHANGE FOR IAB WITH SOIL INTERACTION WITH RESPECT TO IAB WITHOUT SOIL INTERACTION FOR DEAD LOAD + LIVE LOAD CONDITION

		Difference		% Change
Deflection	End Girder	1.34	mm	2.54
	Central Girder	1.94	mm	4.02
Shear Force in Longitudinal Girders	End Girder	0.88	kN	0.14
	Central Girder	3.75	kN	0.72
Bending Moment in Longitudinal Girders	End Girder	-43.9	kN-m	1.57
	Central Girder	-58.3	kN-m	2.47
Bending Moment in Deck Slab	End Plate	-0.57	kN-m/m	2.27
	Centre Plate	0.34	kN-m/m	1.55

There is slight increase in deflection, shear force and bending moments (both positive and negative) in longitudinal girders and deck slab for IAB with soil interaction compared to IAB without soil interaction for both the dead load and live load condition given in table 1 and 2.

6 CONCLUSIONS

Following are the conclusions based on the study:

1) The maximum deflection in longitudinal girder of integral abutment bridge (IAB) is observed to be more when soil interaction is taken into account for all temperature ranges studied. Similar are the observations for shear force and bending moment in deck slab. This is due to effect of restraint provided by stiffness of soil behind the abutment and around the piles.
2) There is no significant variation in bending moment, shear force and deflection in the longitudinal girder and deck slab for a particular temperature change for IAB with and without soil interaction.
3) It is observed that by changing the soil properties behind the abutment and around the piles does not affect significantly the performance of deck slab in terms of bending moment, shear force and deflection.
4) The bending moment and deflection in deck slab and girders increases linearly with increase in temperature.
5) The moments on deck slab increase with increase in temperature for integral abutment bridges.

ISSN 2229-5518

REFERENCES

[1] Alok Bhowmick, "Design and Detailing of Integral Bridges: Suggested Guidelines" *Indian Concrete Journal,* Vol 79, No 9, pp.43-50, Sept 2005.

[2] Eugenia Roman , Yasser Khodair and Sophia Hassiotis, "Design Details of Integral Bridges" *Dept. of Civil Engineering And Ocean Engineering, Stevens Institute Of Technology, Hoboken N.J.*

[3] Murat Dicleli, Suhail M. Albhaisi,"Performance Of Abutment Backfill System Under Thermal Variations In Integral Bridges Built On Clay" *Engineering Structures,* Vol 26, pp. 949-962, Feb 2004.

[4] Shehab Mourad & Sami W.Tabsh, "Deck Slab Stresses In Integral Abutment Bridges" *Journal of Bridge Engineering* Vol.4 No.2 May 1999.

[5] Murat Dicleli, "Simplified Model for Computer-Aided Analysis of Integral Bridges" *J. Bridge Engg.* Volume 5, Issue 3, Pp. 240-248, Aug 2000.

[6] Susan Faraji, John M.Ting, Daniel S. Crovo and Helmut Ernst, "Nonlinear Analysis of Integral Bridges: Finite Element Model" *Journal of Geotechnical & Geo environmental Engg*, Vol 127, No 5, May 2001.

[7] George L. England and Neil C. M. Tsang, "Design of Soil Loading For Integral Bridges" *The Indian Concrete Journal*, Vol 79, No.9, pp.75-84, Sept 2005.

[8] D.D Girton, T.R. Hawkinson & L.F. Greimann, "Validation of Design Recommendations for Integral – Abutment Piles" *Journal of Structural Engineering,* Asce, Vol 117, No.7 .July 1991.

[9] Edward P. Wasserman "Integral Abutment Practices in the United States" *Indian Concrete Journal*, Vol 79, No.9, pp. 56-65, Sept 2005.

[10] Murat Dicleli, Suhail M. Albhaisi, "Maximum Length Of Integral Bridges Supported On Steel H-Piles Driven In Sand" *Engineering Structures,* Volume 25, Issue 12, Pg 1491-1504, Oct 2003.

[11] Harish Kulkarni, "Parametric Study of Integral Abutment Bridge with Soil-Structure Interaction", M.Tech Thesis, Gogte Institute of Technology, Belgaum, India, 2011.

[12] IRC 5-1998, "Standard Specifications And Code Of Practice For Road Bridges" Section I, General Features of Design, The Indian Roads Congress, New Delhi, India, 1998.

[13] IRC 6-2000, "Standard Specifications and Code of Practice for Road Bridges", Section II, loads and stresses, The Indian Roads Congress, New Delhi, India, 2000.

[14] "Bridge Design using the STAAD.Pro/Beava", IEG Group, Bentley Systems, Bentley Systems Inc., March 2008.